

**Magnetic Fields in the Universe:
From Laboratory and Stars to Primordial Structures
Cargese, France, 5 - 9 October, 2015**

Magnetic Field in the Outer Heliosphere and Beyond

N.V. Pogorelov

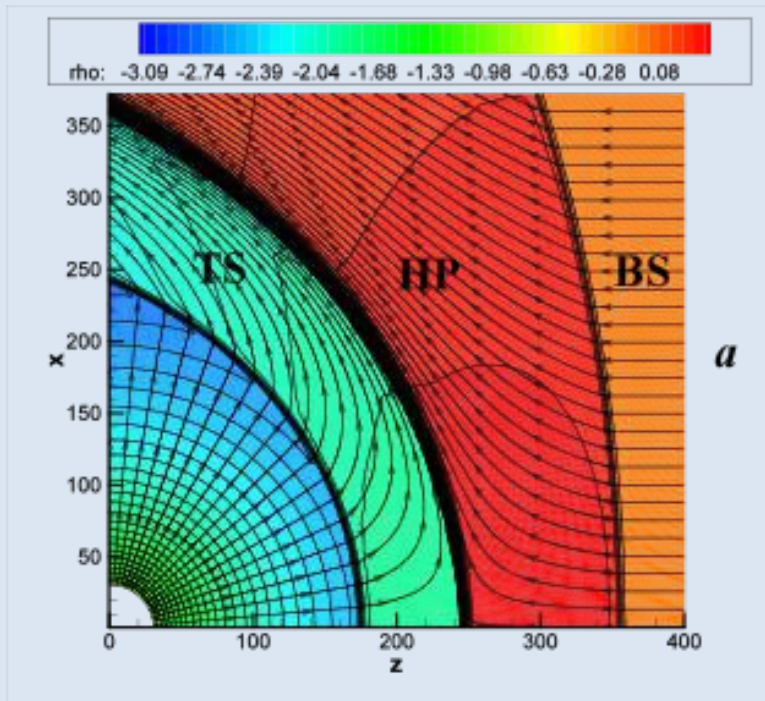
**University of Alabama in Huntsville, Department of Space Science and
Center for Space Plasma and Aeronomic Research**

Outline

1. **Key Challenges.**
2. **Why it matters?**
3. **Magnetic field and charge exchange effects.**
4. **Hydrogen deflection plane**
5. **Transition to turbulence in the inner heliosheath.**
6. **Mixing of the SW and LISM plasmas the heliopause.**
7. **Heliotail and TeV cosmic ray anisotropy.**

Key Challenges

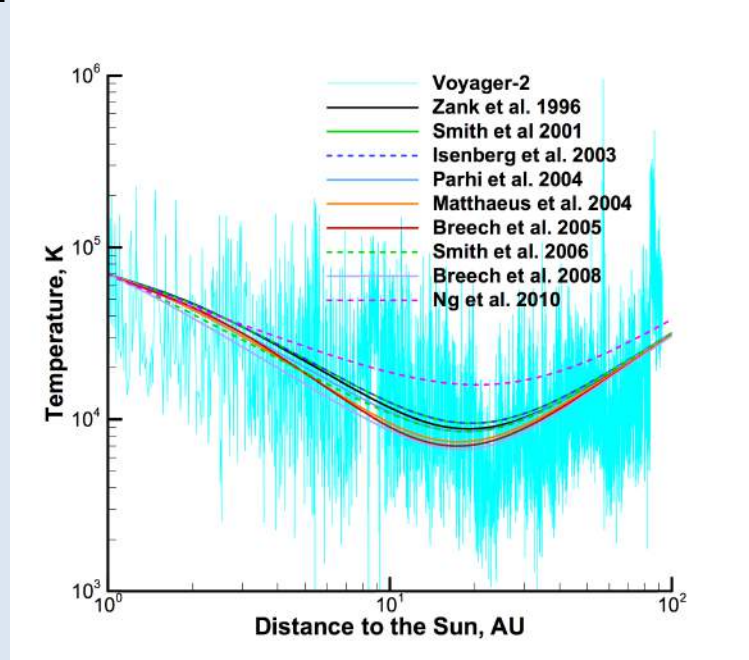
1. Flows of partially ionized plasma are frequently characterized by the presence of both thermal and nonthermal populations of ions and neutral atoms. This occurs, e. g., in the outer heliosphere - the part of interstellar space beyond the solar system whose properties are determined by the solar wind (SW) interaction with the local interstellar medium (LISM).



The Sun is at the origin, the LISM flow is from the right to the left. Their interaction creates a heliospheric termination shock, a heliopause, and a bow wave that may include a sub-shock inside its structure.

The LISM is partially ionized (there are maybe 3 times more H atoms than H^+ ions, hence charge exchange becomes of importance.

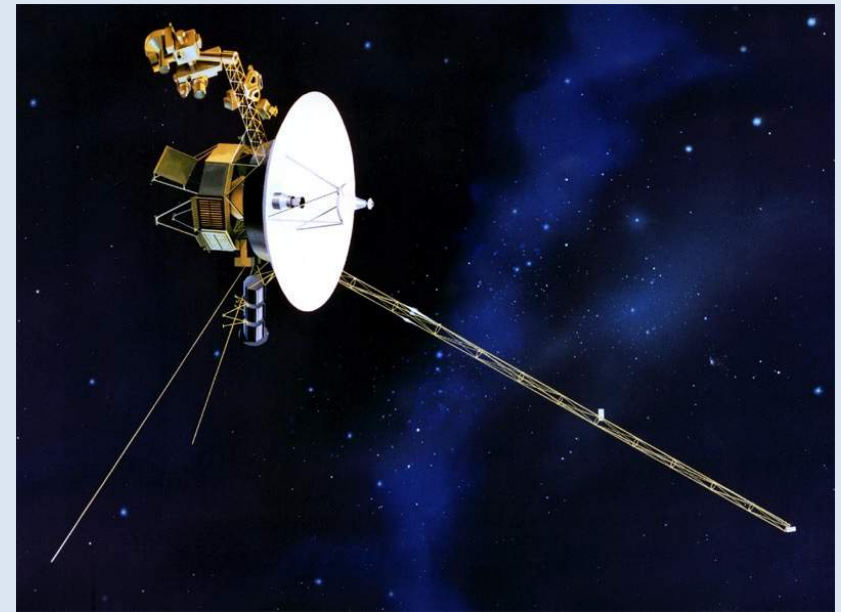
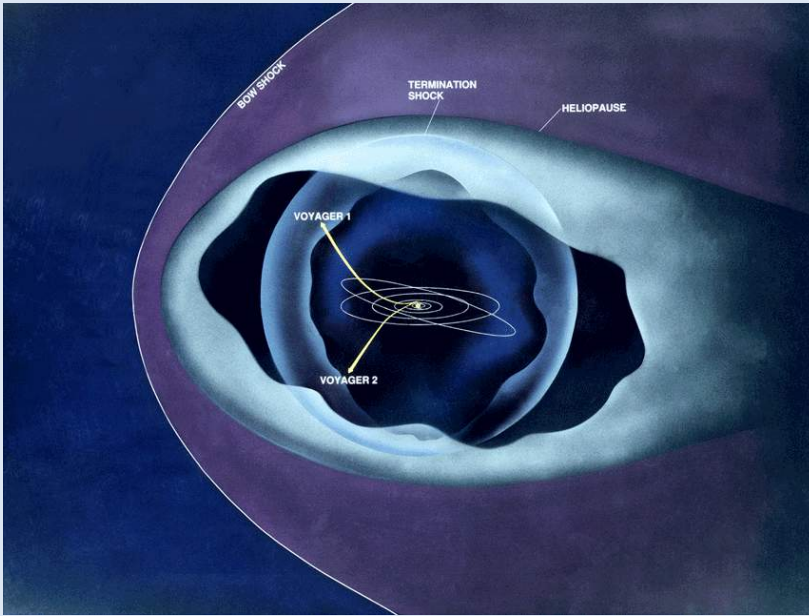
2. Understanding the behavior of such flows requires that we investigate a variety of physical phenomena: charge-exchange processes between neutral and charged particles, the birth of pick-up ions (PUIs), the origin of energetic neutral atoms (ENAs), production of turbulence, instabilities and magnetic reconnection, etc. Collisions between atoms and ions in the heliospheric plasma are so rare that they should be modeled kinetically. PUIs, born when LISM neutral atoms experience charge-exchange with SW ions, represent a hot non-equilibrium component and also require special treatment.



From Kryukov et al. (2012): turbulence produced by non-thermal ions heats up the solar wind, which otherwise would have cooled down with heliocentric distance adiabatically.

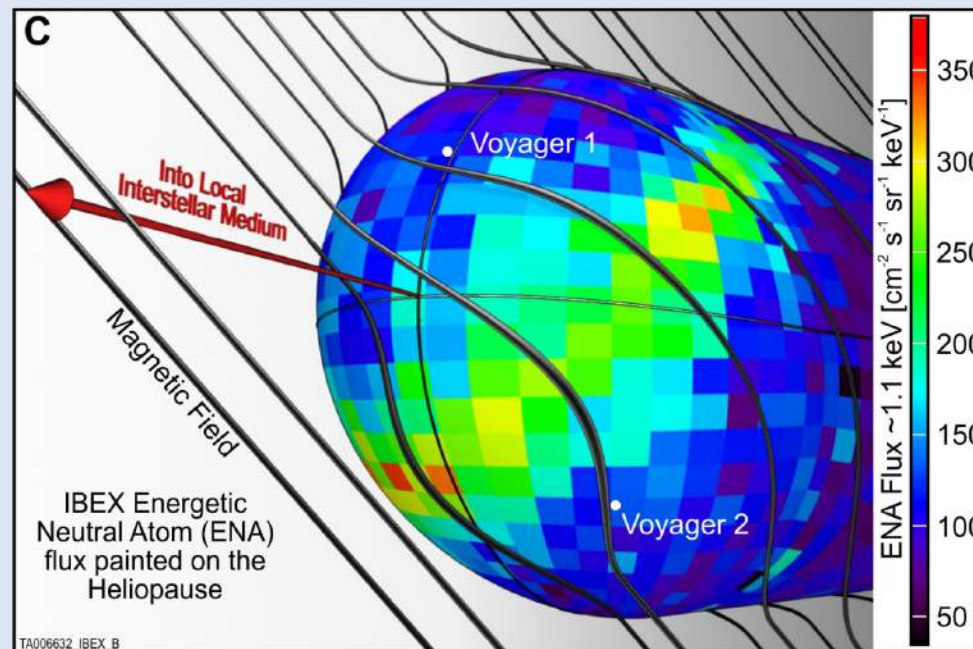
3. The solar wind perturbs the LISM substantially: about 1000 AU upwind and 10,000 AU in the tail. This perturbation affects TeV cosmic rays and may be an explanation of their observed anisotropy.
4. To address these problems, we have developed a tool for self-consistent numerical solution of the MHD, gas dynamics Euler, and kinetic Boltzmann equations. Our Multi-Scale Fluid-Kinetic Simulation Suite (MS-FLUKSS) solves these equations using an adaptive-mesh refinement (AMR) technology. The grid generation and dynamic load balancing are ensured by the Chombo package.

Why it matters?



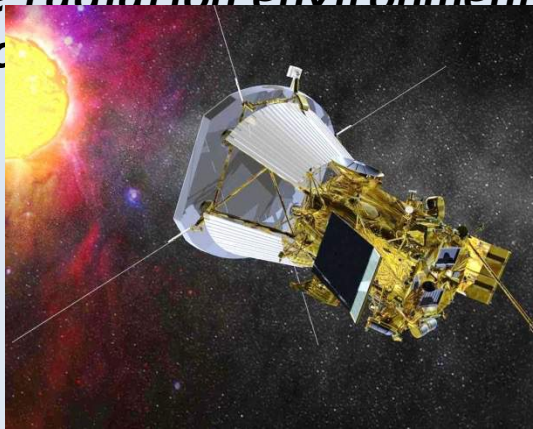
Voyager 1 and *2* (*V1* and *V2*), PI Edward C. Stone, crossed the heliospheric termination shock in December 2004 and in August 2007, respectively (Stone et al., 2005, 2008). After more than 37 years of historic discoveries, *V2* is approaching the heliopause, while *V1* in August 2012 (Stone et al., 2013) penetrated into the LISM and measures its properties directly. They acquire often puzzling information about the local properties of the SW and LISM plasma, waves, energetic particles, and magnetic field, which requires theoretical explanation. In the next few years, the heliospheric community has a unique chance to analyze and interpret Voyager measurements deriving breakthrough information about physical processes occurring more than 1.2×10^{10} miles from the Sun. Illustrations courtesy of NASA at

Our team has proposed a quantitative explanation to the sky-spanning “ribbon” of unexpectedly intense flux of ENAs detected by the Interstellar Boundary Explorer (IBEX, PI David J. McComas). Our physical model makes it possible to constraint the direction and strength of the interstellar magnetic field (ISMF) in the near vicinity of the global heliosphere (Heerikhuisen & Pogorelov, 2011; Heerikhuisen et al, 2014, 2015; Zirnstein et al., 2014, 2015; Pogorelov et al., 2011) . For the next 5–10 years, heliophysics research is faced with an extraordinary opportunity to use *in situ* measurements from Voyagers and extract information about the global behavior of the heliosphere through ENA observations by IBEX.



From McComas et al. (2009)

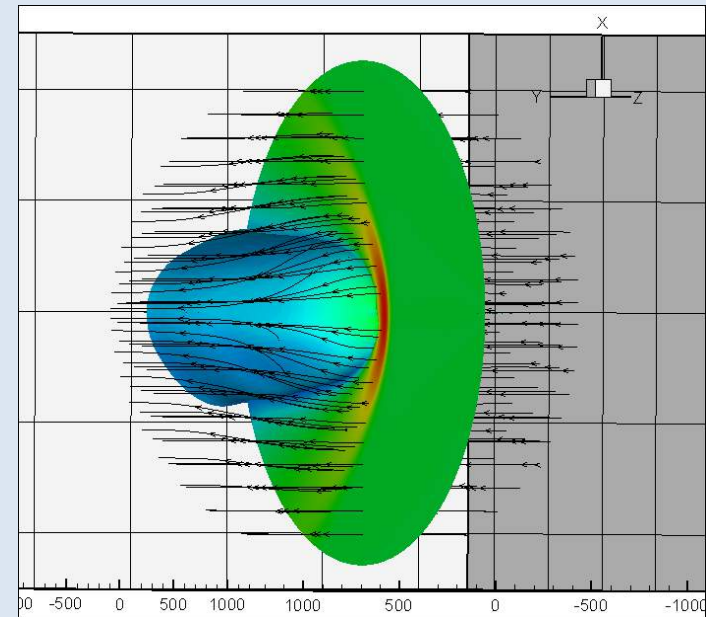
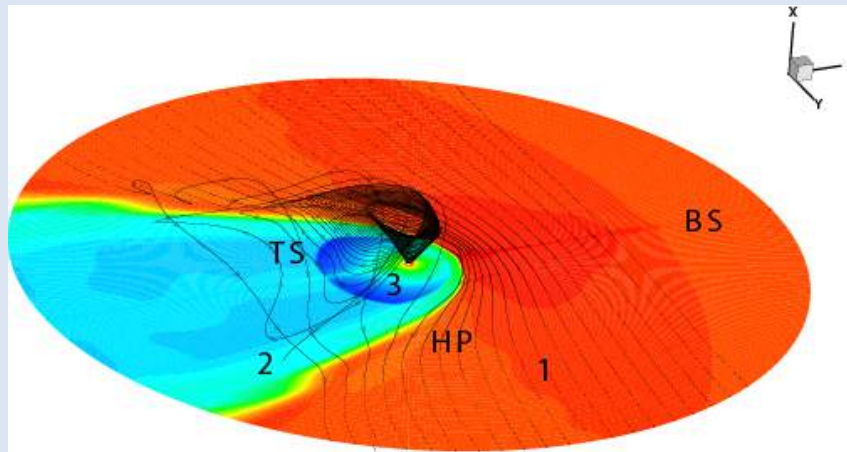
From the SPP official web site <http://solarprobe.gsfc.nasa.gov/>: “Solar Probe Plus will be an extraordinary and historic mission, exploring what is arguably the last region of the solar system to be visited by a spacecraft, the Sun’s outer atmosphere or corona as it extends out into space. Solar Probe Plus will repeatedly sample the near-Sun environment, revolutionizing our knowledge and understanding of coronal heating and of the origin and evolution of the solar wind and answering critical questions in heliophysics that have been ranked as top priorities for decades. Moreover, by making direct, in-situ measurements of the region where some of the most hazardous solar energetic particles are energized, Solar Probe Plus will make a fundamental contribution to our ability to characterize and forecast the radiation environment in which future space explorers will work and



Artist’s view of SPP from <https://www.cfa.harvard.edu/sweap/>

Solar Wind Electrons, Alphas, and Protons (SWEAP) instrument (PI Justin Kasper) onboard SPP, to be launched in 2018, will directly measure the properties of the plasma in the solar atmosphere. In particular, the time-dependent distribution functions will be measured, which requires the development of sophisticated numerical methods to interpret them.

Three-dimensional structure of the heliosphere in the presence of the IMF and ISMF



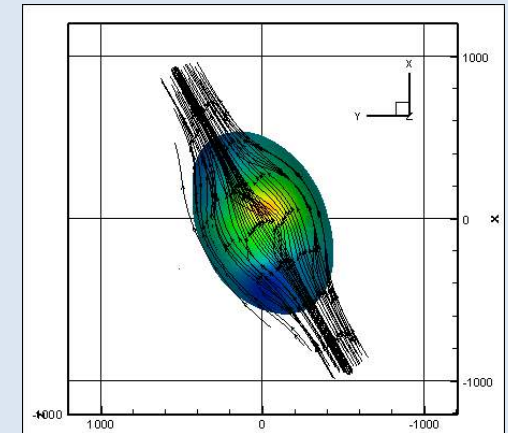
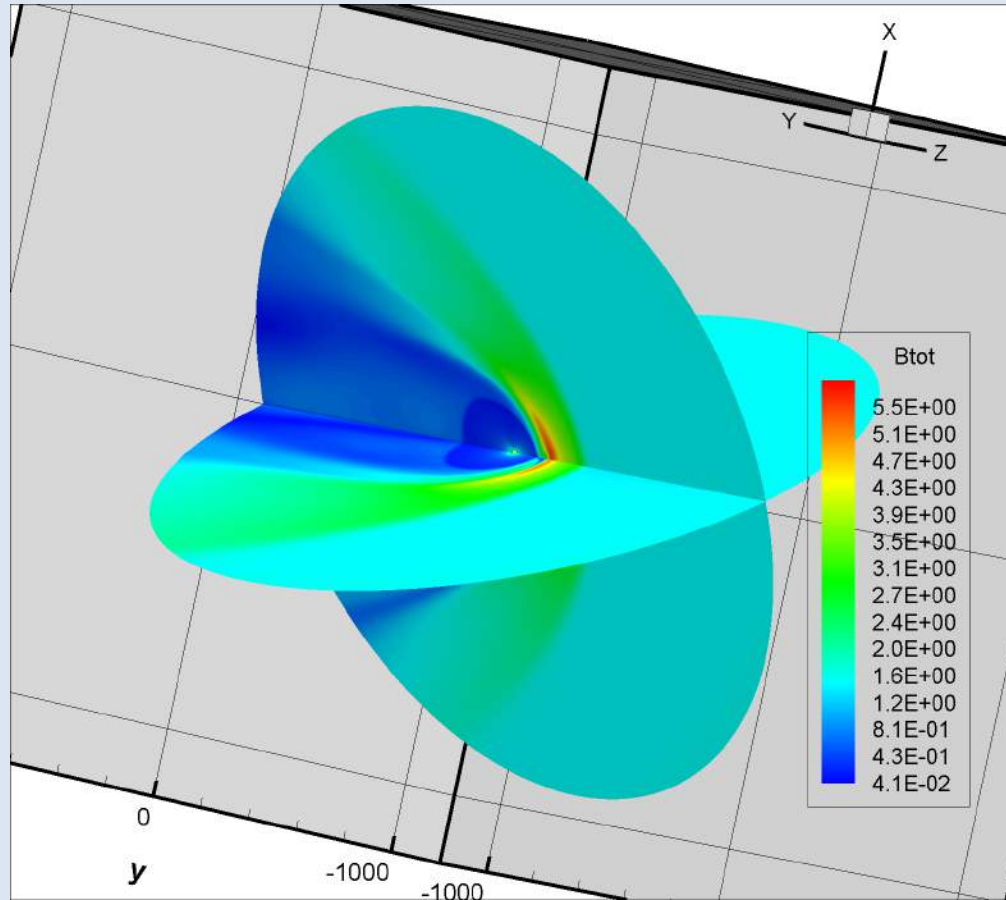
**ISMF draping around the HP and an IMF spiral:
ISMF is perpendicular to the LISM velocity vector
and parallel to the ecliptic plane**

**Magnetic pressure exerted
perpendicular to the magnetic field
direction compresses the
heliopause in the north-south
direction**

From Pogorelov, Zank & Ogino (2004)

ISMF perpendicular to the LISM velocity and tilted 60° to the ecliptic plane

Cross-sections of the widest and narrowest flaring of the heliopause

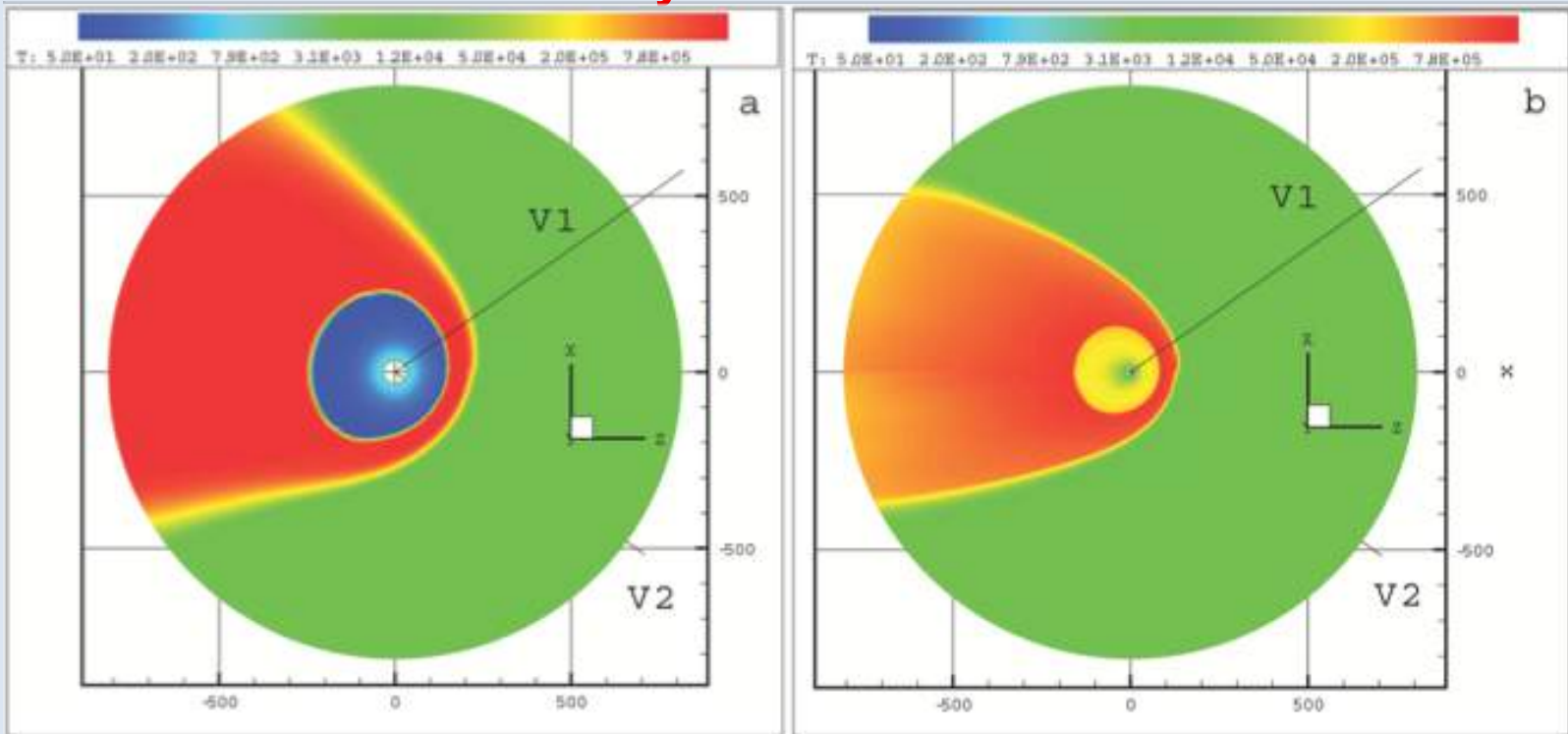


The HP rotates under the action of magnetic pressure and aligns with the BV -plane (the plane formed by B_∞ and V_∞)

Initially planar HCS bends and rotates with respect to the z-axis, which is parallel to V_∞ .

From Pogorelov, Zank & Ogino (2004)

The angle between the ISMF and the LISM velocity is 45° and $B_\infty = 2.5 \mu\text{G}$ (BV-plane coincides with the meridional plane).
North-south asymmetries of the TS and HP.



No neutrals, no IMF

With IMF and $n_{\text{H}\infty} = 0.15 \text{ cm}^{-3}$

Asymmetry of discontinuities with respect to the ecliptic plane becomes substantially less pronounced! V1-V2 asymmetry: 11 AU without neutrals and 2 AU with charge exchange. Neutral H density increase further symmetrizes the heliosheath.

Heliospheric current sheet / sectors in the heliosheath

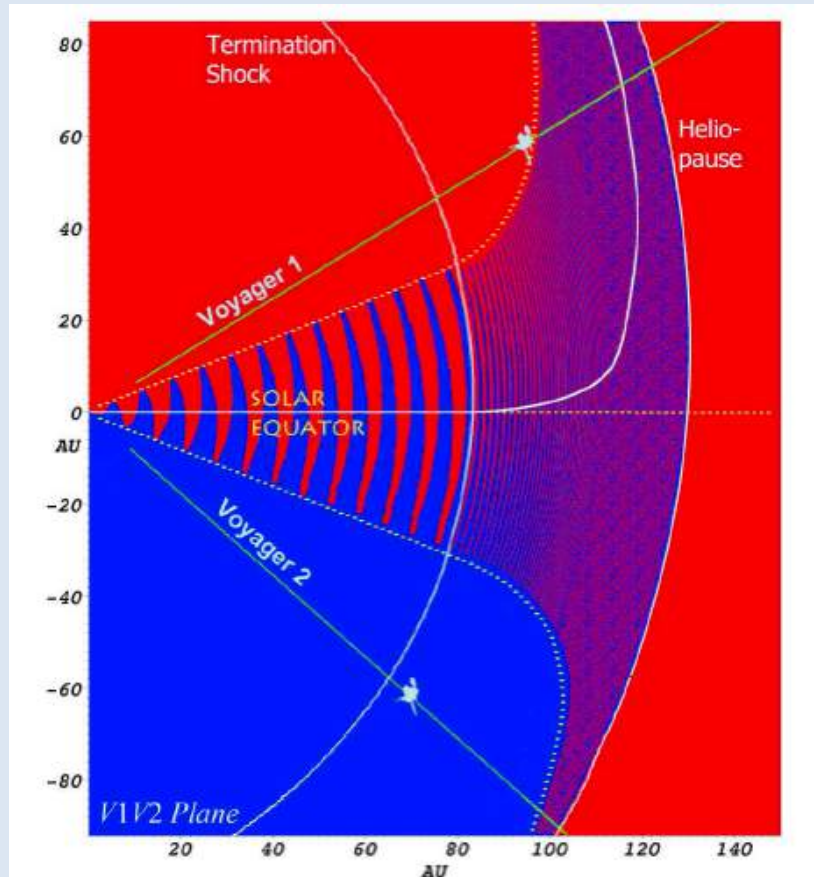


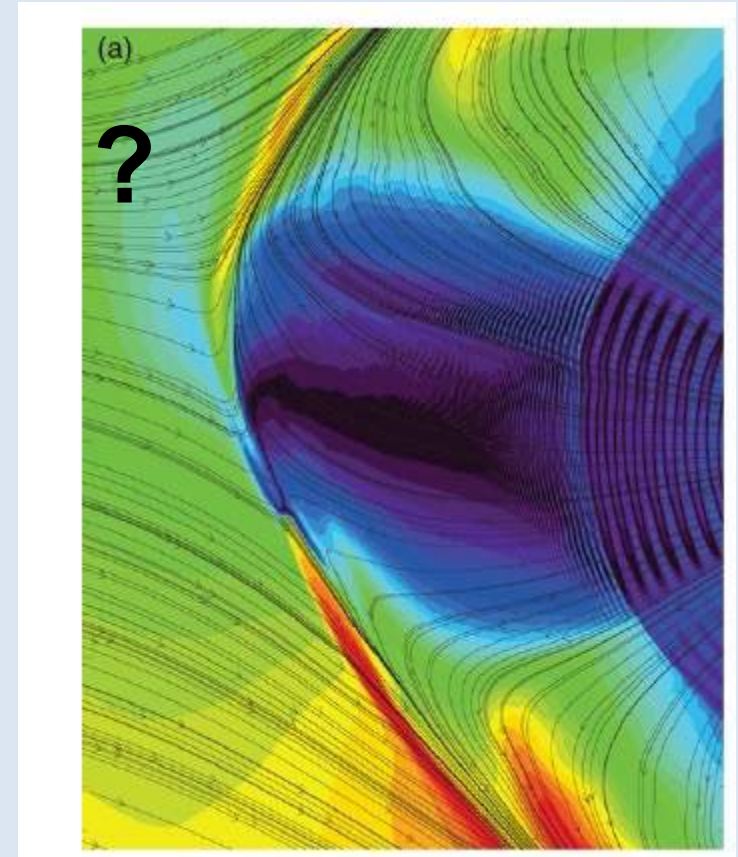
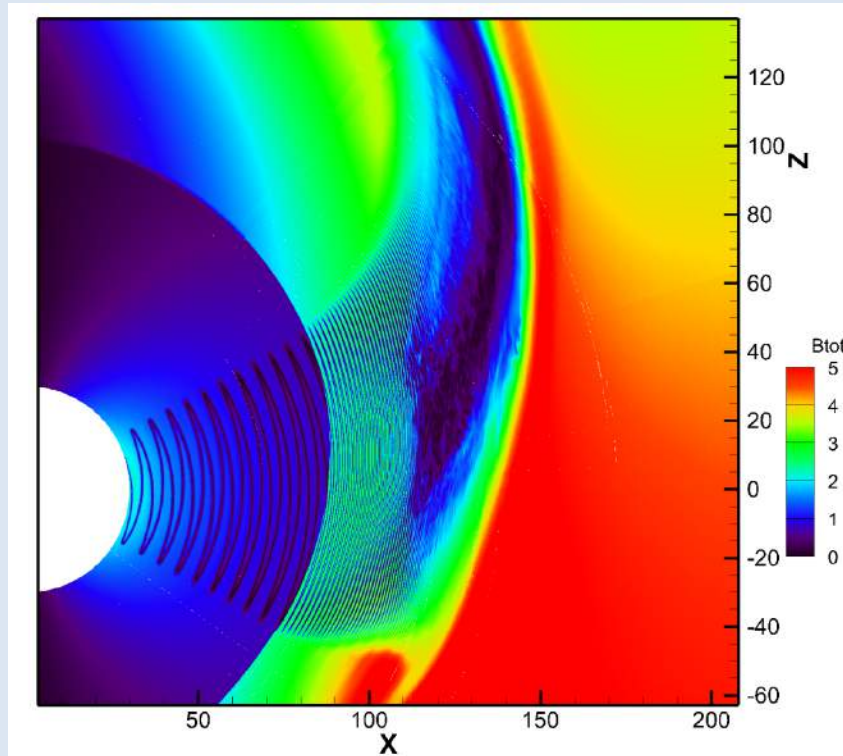
Figure 5: The HCS shape in the plane formed by the V1 and V2 trajectories.

2 different approaches are pursued:

- (1) keep the dipolar field as is and let it dissipate due to turbulence near the heliopause;
- (2) assume a unipolar field and assign the signs afterwards.

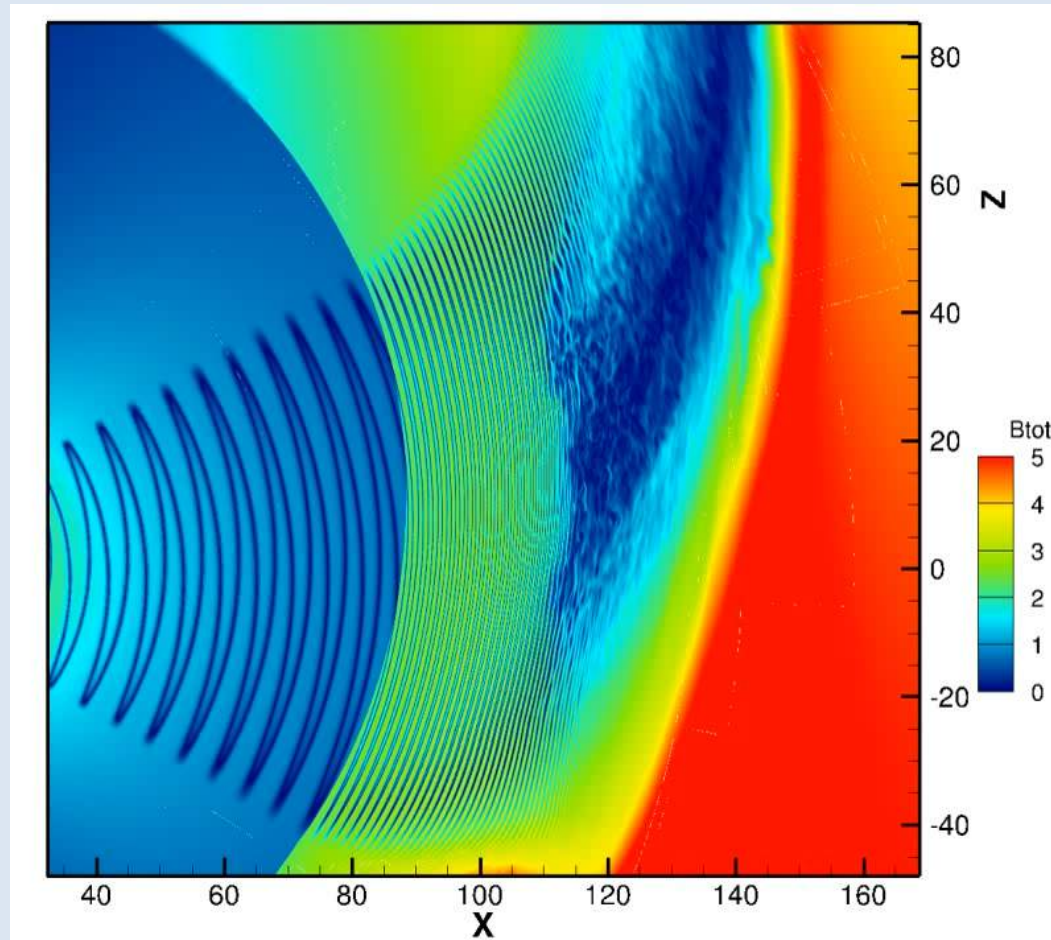
Unipolar HMF simulation of Borovikov et al. (2011). Similar approaches were used by Czechowski et al., Izmodenov et al., and Florinski et al.

Transition to chaotic behavior in the IHS (parameters from Opher et al., 2012)



The distribution of $|B|$ using the same color scale: no irregular structures or tangential discontinuities disrupting the heliospheric current sheet are observed

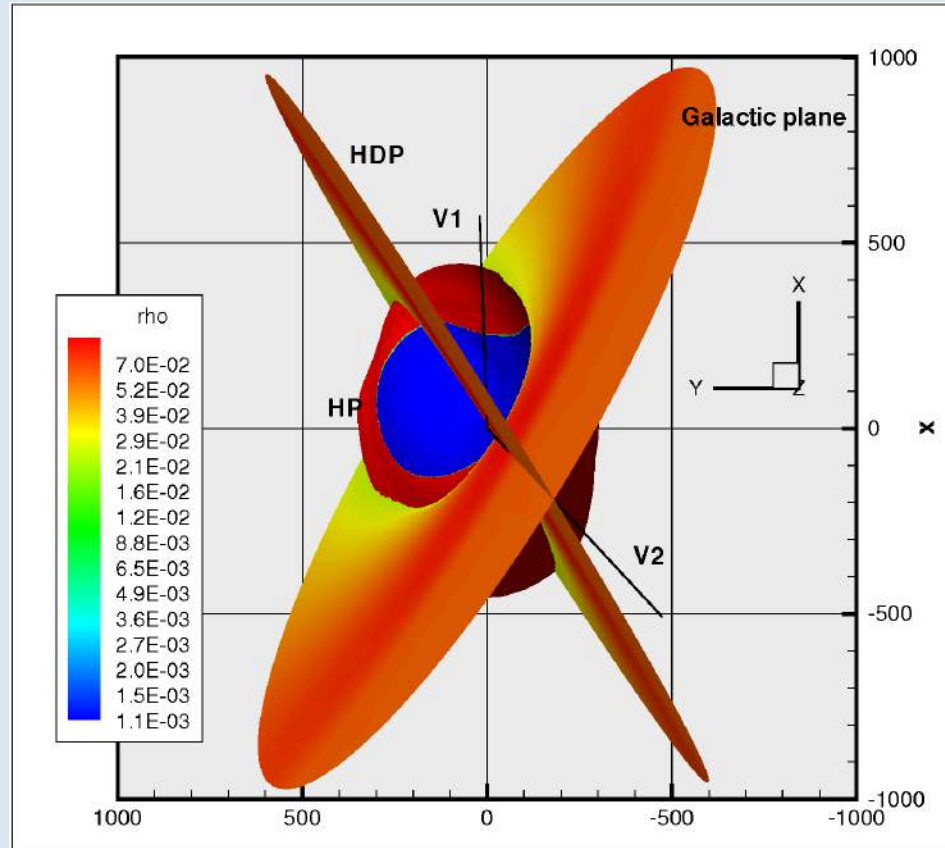
Transition to chaotic behavior in the IHS (Pogorelov et al., 2013)



Evolution of the heliospheric magnetic field in the inner heliosheath: the reason is tearing-mode instability due to numerical dissipation. In reality, such turbulence should occur closer to the heliopause.

The heliopause colored by the sign of B_R , the hydrogen deflection plane, the Galactic plane, and the trajectories of the V1 and V2 spacecraft

Pogorelov,
Heerikhuisen,
Zank (2008)



The HP is not symmetric with respect to the BV-plane!

H-atom deflection almost entirely in the BV-plane!

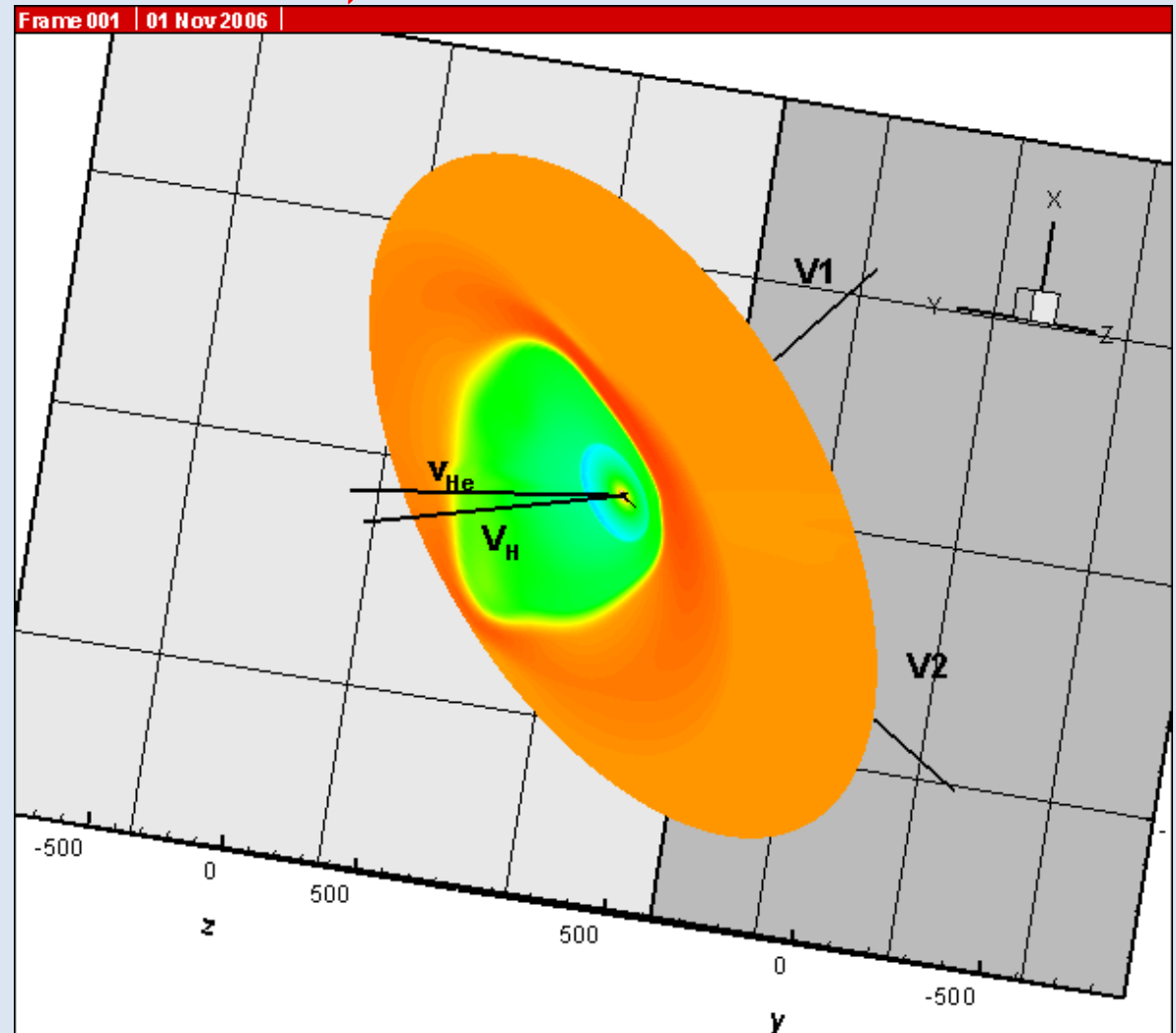
BV-plane parallel to the HDP, B_∞ at 30° to V_∞ ($B_\infty = 3 \mu\text{G}$), $n_{\text{H}\infty} = 0.15 \text{ cm}^{-3}$

The LISM parameters are chosen to fit the IBEX ribbon data.

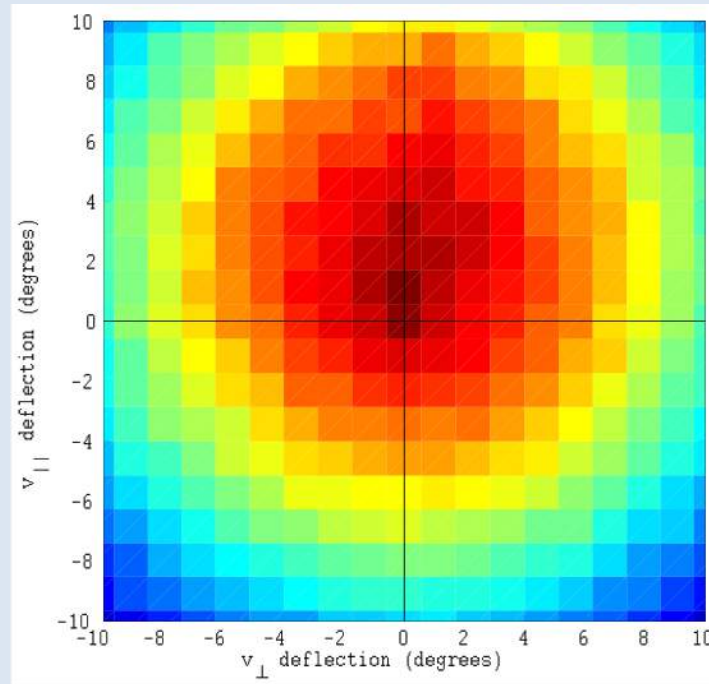
ISMF in the HDP: Direction of the neutral hydrogen velocity in the inner heliosphere as a possible interstellar magnetic field compass (Izmodenov et al., 2005; Pogorelov & Zank, 2006; Pogorelov et al., 2008, 2009)

According to the SOHO SWAN experiment (Lallement et al, 2005, 2010), there is an angle of about 4° between the neutral He and neutral H flow velocity vectors in the inner heliosphere.

The vectors B_∞ and V_∞ define the BV -plane, which supposedly is nearly parallel to the HDP (exactly parallel in Izmodenov et al. 2005).



Two-dimensional distribution of the neutral H deflections in the plane perpendicular to V_∞ (from Pogorelov et al., 2008)



B_∞ in the RL-plane at 30° to the LISM velocity and the ecliptic plane.

To determine the deflection on H-atoms, we collected statistics within a 45-degree cone around the LISM flow vector within the supersonic solar wind. The combined population LISM neutrals are deflected about 3.8° in the BV-plane and about 0.05° perpendicular to this plane.

IBEX Ribbon Defines the Position of the BV-plane

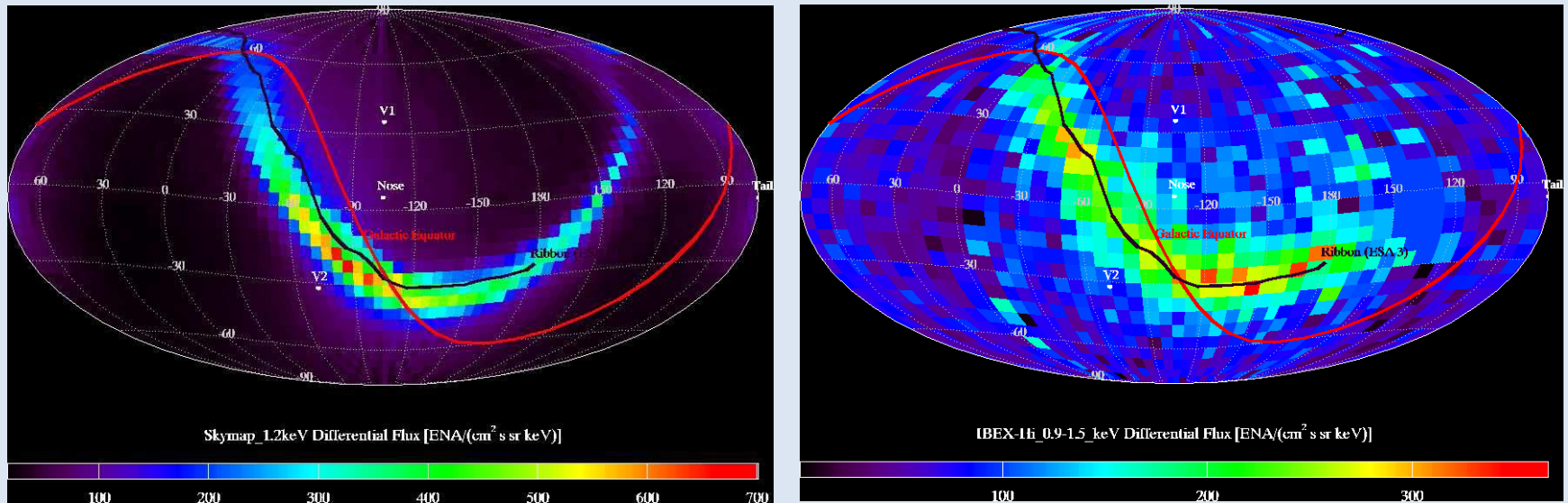


FIGURE 1. All-sky maps of simulated (left) and observed (right) ENA fluxes at 1.1 keV. The simulation uses a $\kappa = 1.63$ spectral index for IHS protons, and we have assumed that all PUIs retain partial shell distributions long enough to re-neutralize before they isotropize. The red curve is the galactic plane, and a best fit to the observed ribbon is shown as a black line. Note that the ribbon shifts down slightly at high energies. Units of ENA flux are $(\text{cm}^2 \text{ s sr keV})^{-1}$.

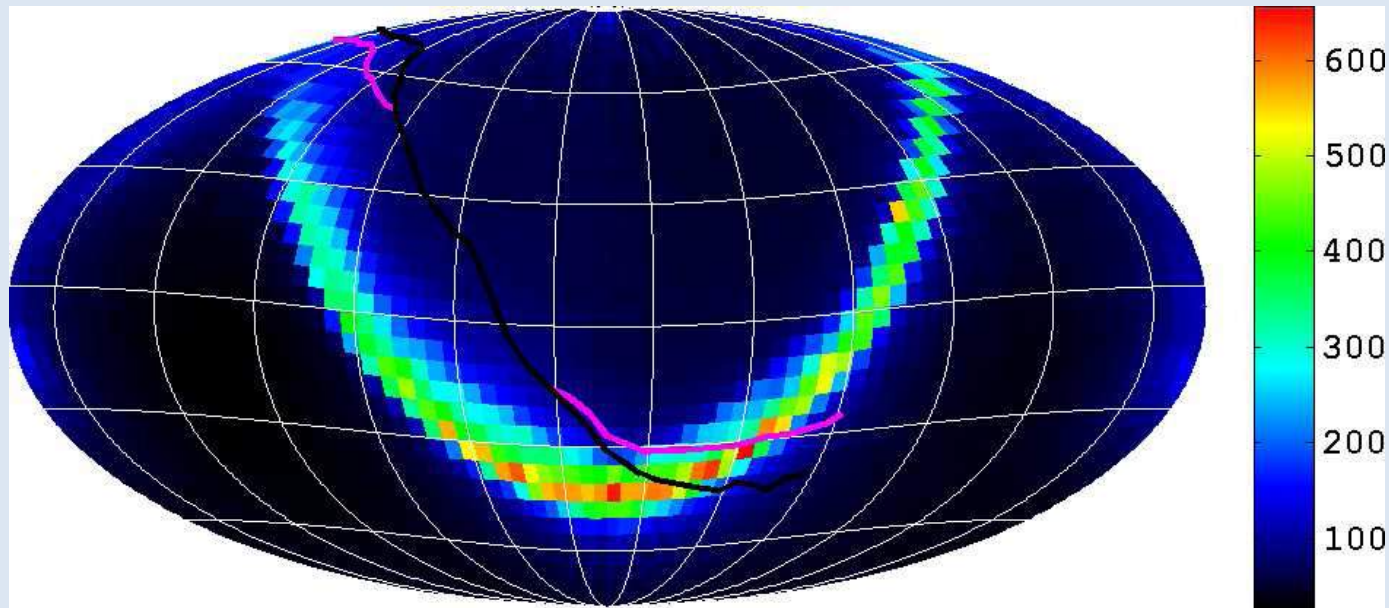
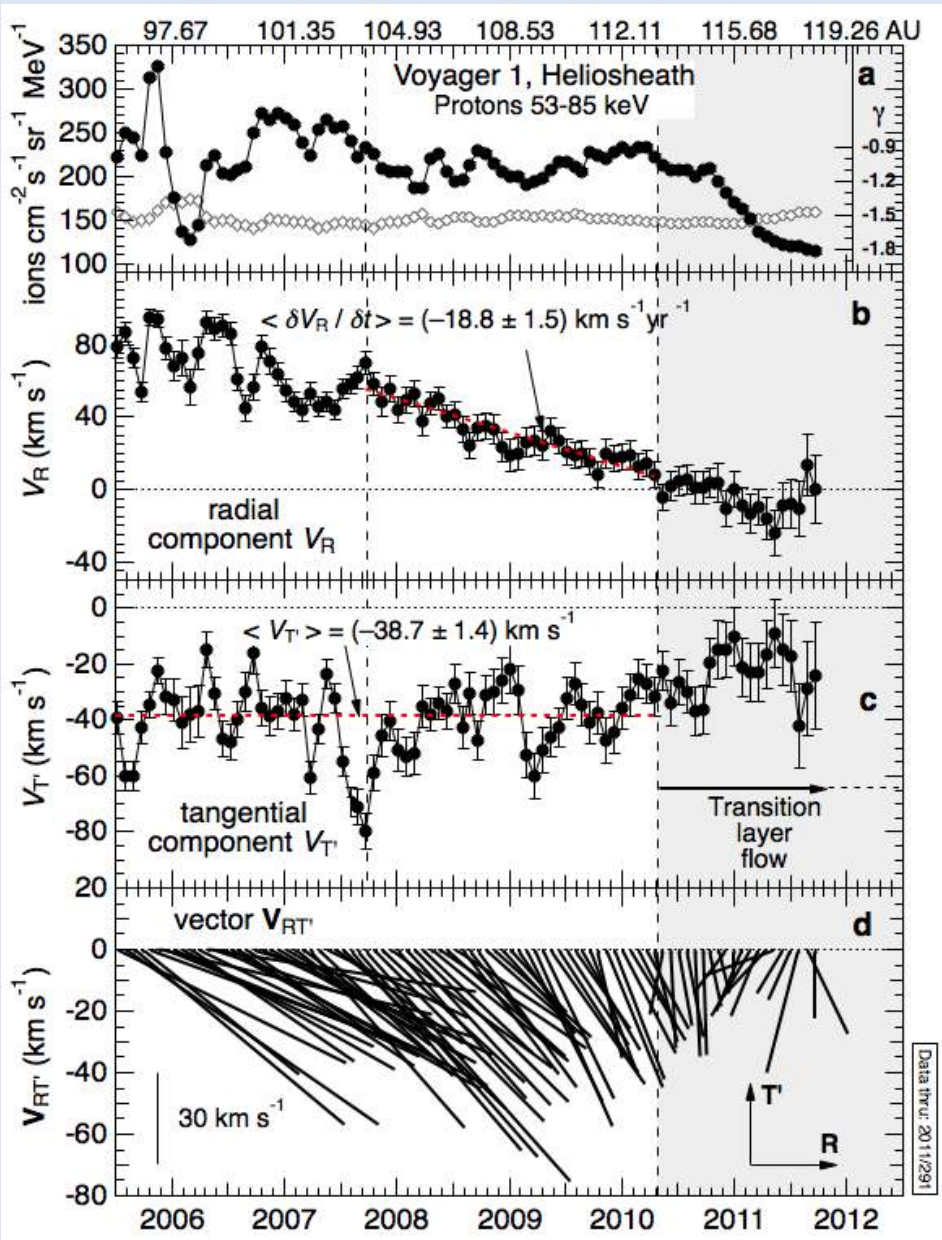


FIGURE 2. An all-sky map of simulated ENA fluxes at 1.1 keV. The LISM parameters are taken from [42]. The simulation uses a $\kappa = 1.63$ spectral index for IHS protons. As seen from the figure, the difference between the simulated and observational results is large for a 30° offset between the HDP and the $B-V$ plane. The solid black and pink lines correspond to the best fit of the IBEX data at 4.3 keV and 1.1 keV, respectively

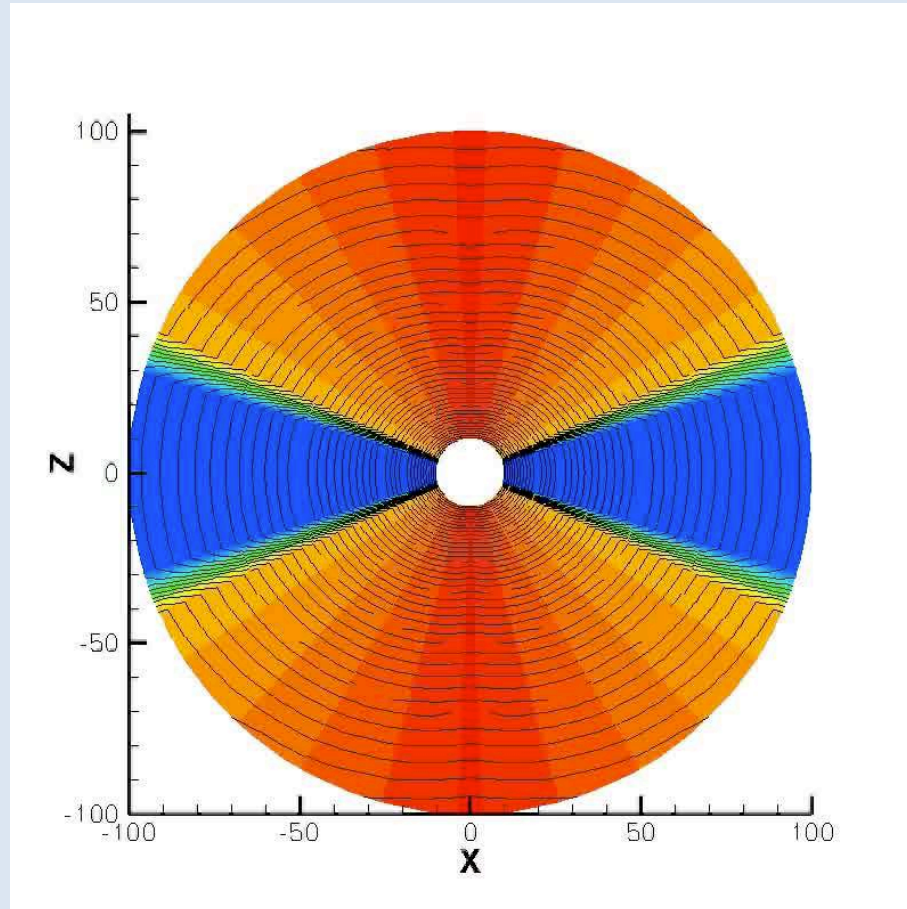
**From Pogorelov et al., 2010 (Annual IAC Proceedings)
 This result was further elaborated in Heerikhuisen & Pogorelov (2011)**



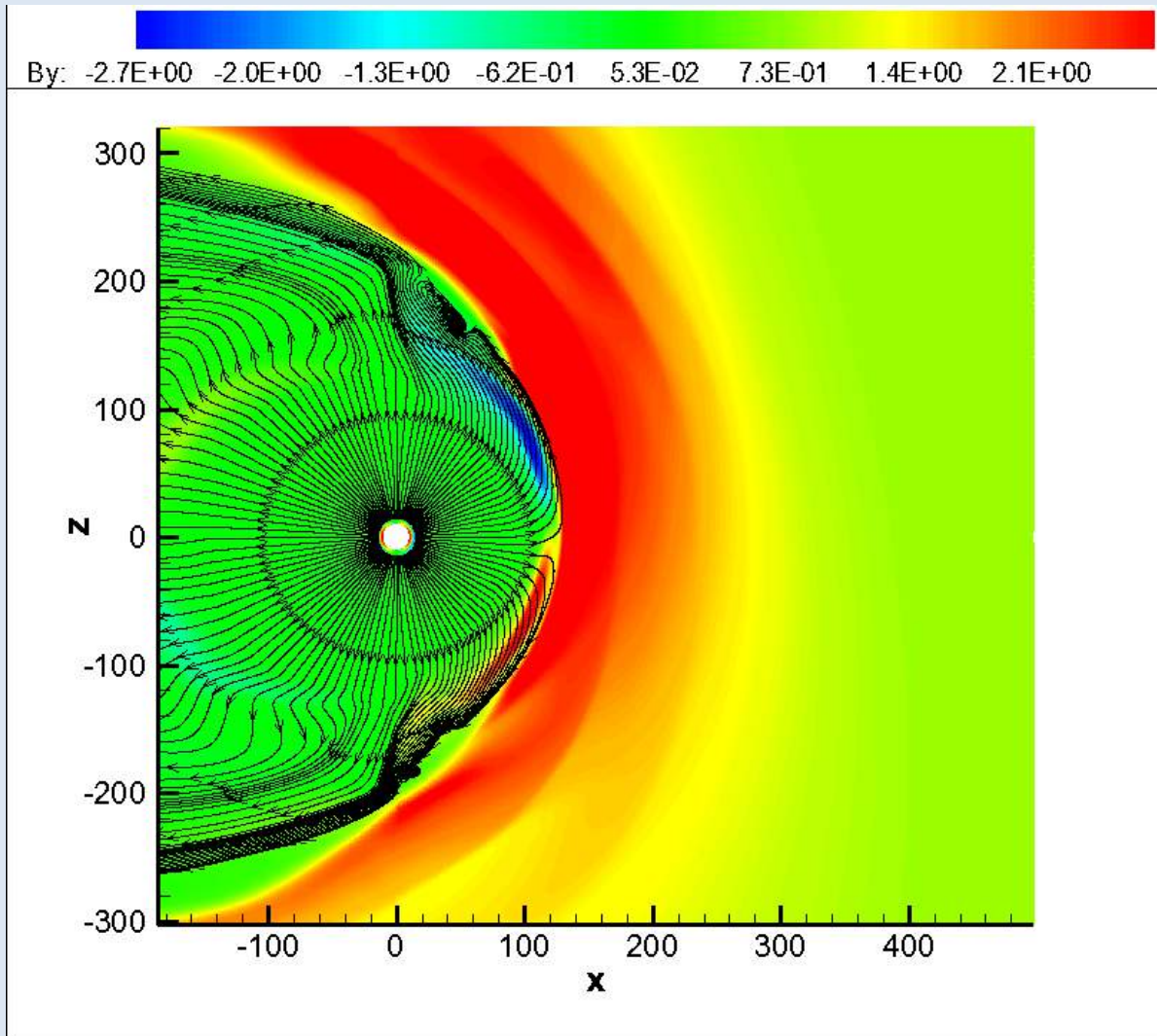
Radial velocity component, derived from the LECP instrument onboard V1, has exhibited gradual decrease since 2007.5 and acquired negative values since the end of 2010 (Krimigis et al., 2011).

This astounding result seemed to be mysterious from a steady-state-solution viewpoint, but was it unexpected by theorists, as was written in *TIME* magazine?

Solar cycle variations of the SW velocity derived from the Ulysses measurements (Pogorelov et al., 2013)

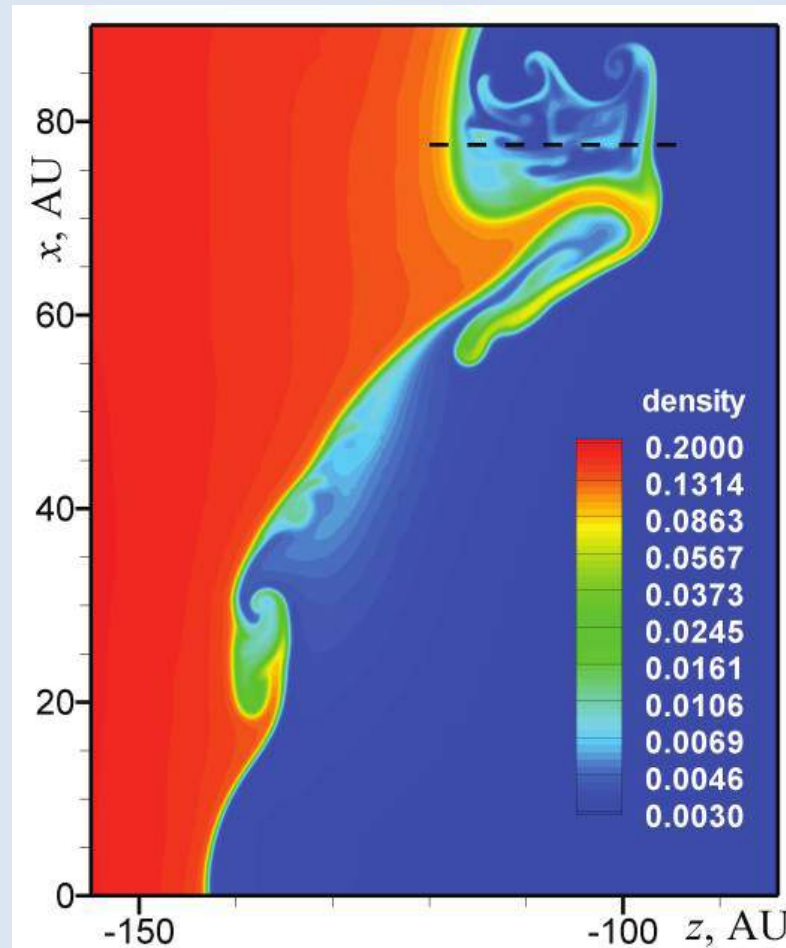


The distribution of the SW radial velocity component in the supersonic region only.



B_y in the meridional plane and SW streamlines

Heliopause Instability May Strongly Affect Its Shape and the Distribution of Quantities in its Vicinity



Mixing of the SW and LISM plasma due to the instability [from Borovikov et al. (2008)].

Parameters for SW-LISM interaction models:

(a) *Solar wind at 1AU:*

$$n_p = 7.4 \text{ cm}^{-3} \quad T = 51100 \text{ K}$$
$$|u| = 450 \text{ km/s} \quad B_r = 35 \mu\text{G} \text{ or } 0 \mu\text{G}$$

(b) The same as (a), but no HMF

(c) The same as (a), but no ISMF

(d) Solar cycle model

Quantity	Slow SW	Fast SW
Number density, n , cm^{-3}	6.9	2.4
Radial velocity component, V , km s^{-1}	450	762
Temperature, T , K	68000	245000
Radial component of the HMF, B_R , μT	3.5	3.5

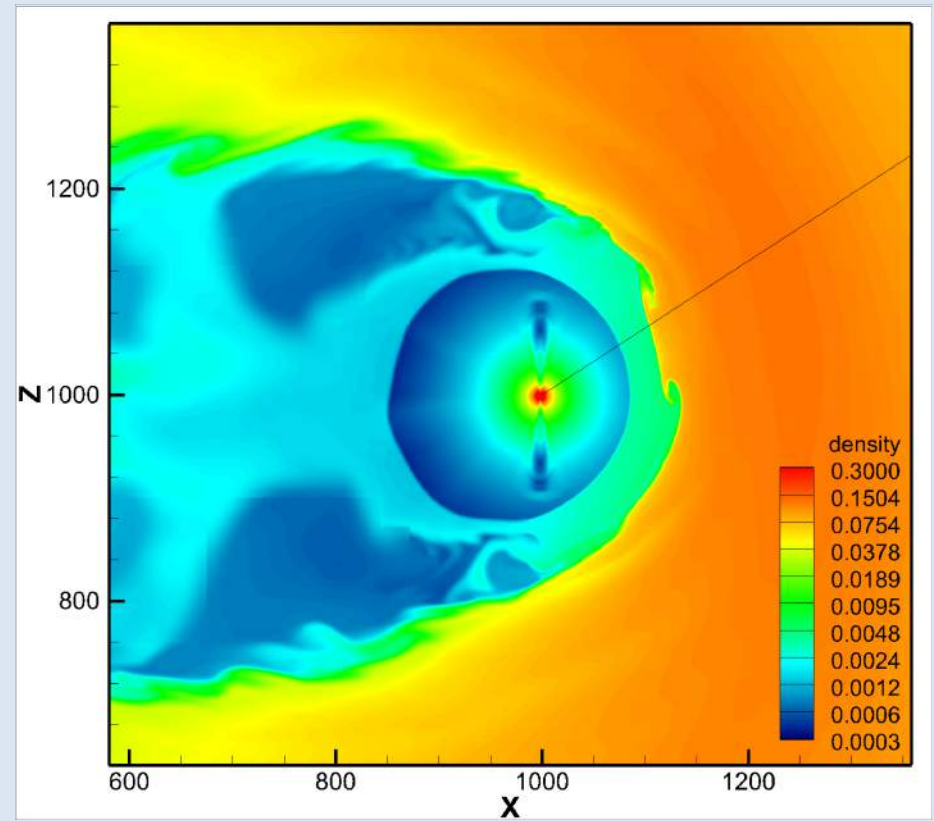
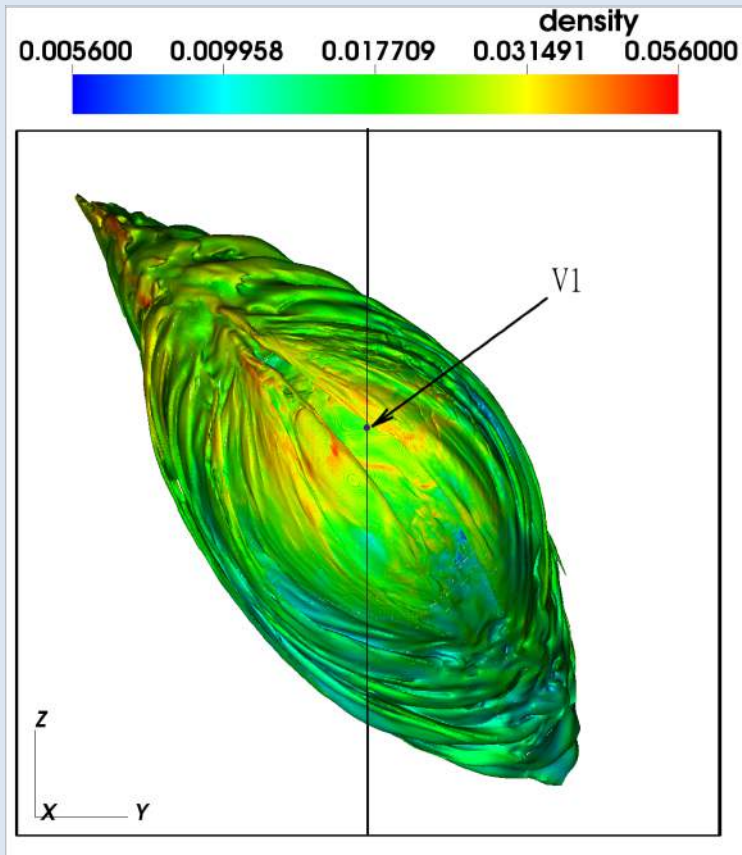
Local Interstellar Medium at 1AU:

$$n_p = 0.08 \text{ cm}^{-3} \quad T = 6200 \text{ K}$$
$$|u| = 23.2 \text{ km/s} \quad B_\infty = 3 \mu\text{G} \quad n_H = 0.21 \text{ cm}^{-3}$$

He direction: $\lambda = 79^\circ, \beta = 4.9^\circ$

IMF direction: $\lambda = 255^\circ, \beta = 44^\circ$

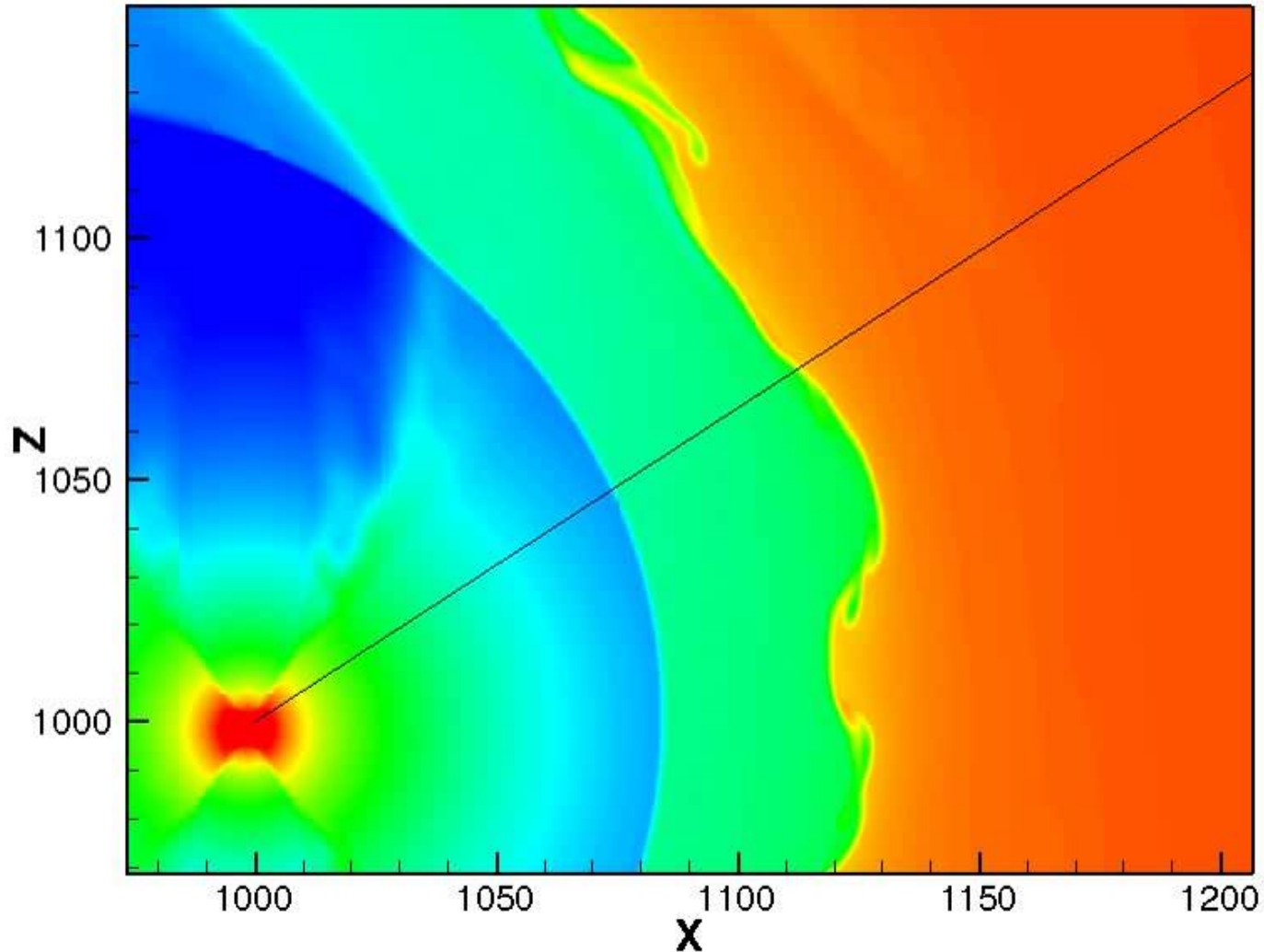
The simulations are performed using a 4-fluid model (one plasma fluid and three neutral atom populations) implemented in Multi-Scale Fluid-Kinetic Simulation Suite (MS-FLUKSS). We use adaptive mesh refinement technique to achieve the resolution of about 0.4 AU in the vicinity of the heliopause



(Right) The frontal view of the HP and **(left)** the plasma density distribution in the meridional plane: solar cycle (Borovikov & Pogorelov, 2014).

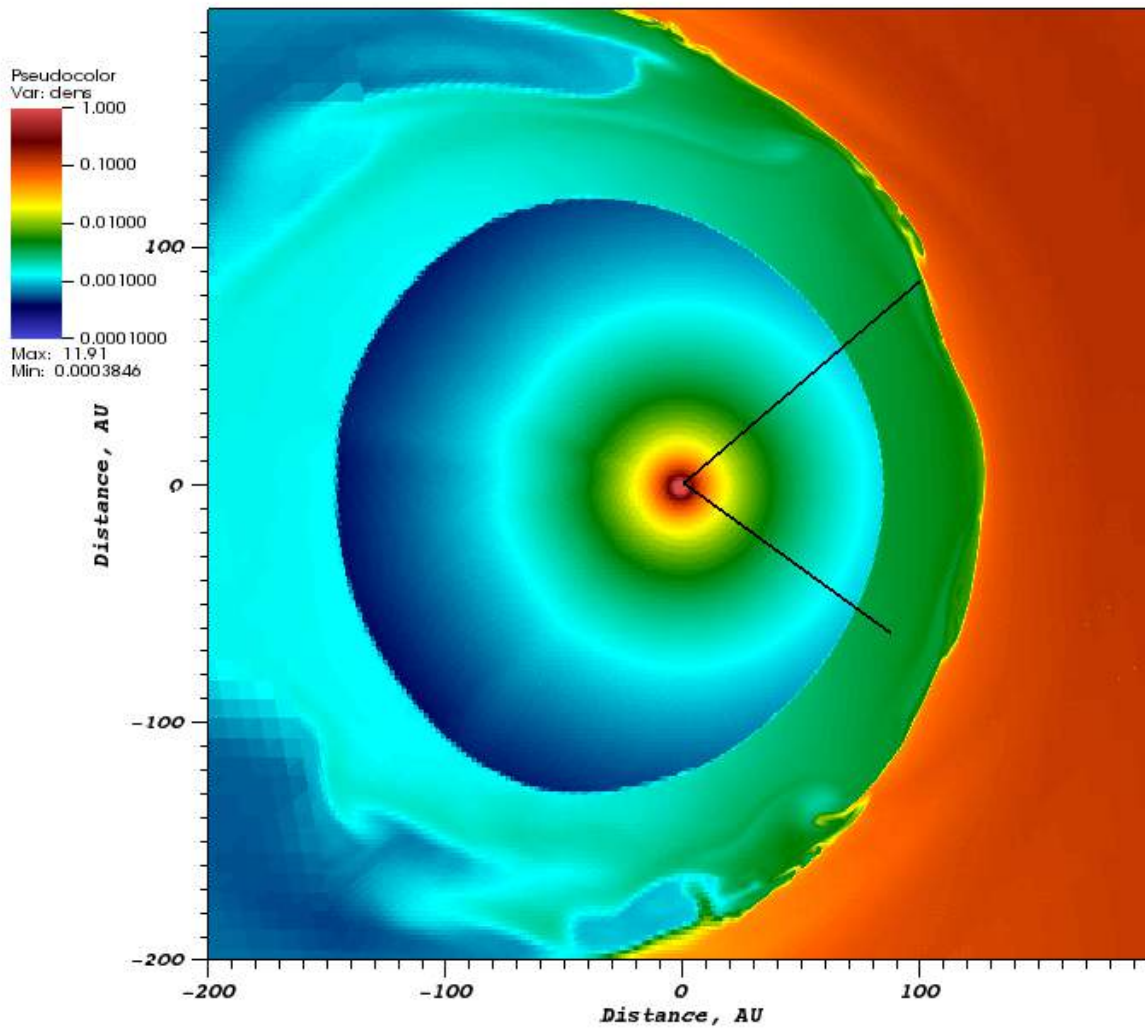


density: 0.0004 0.0007 0.0014 0.0026 0.0048 0.0089 0.0167 0.0310 0.0577 0.1074 0.2000

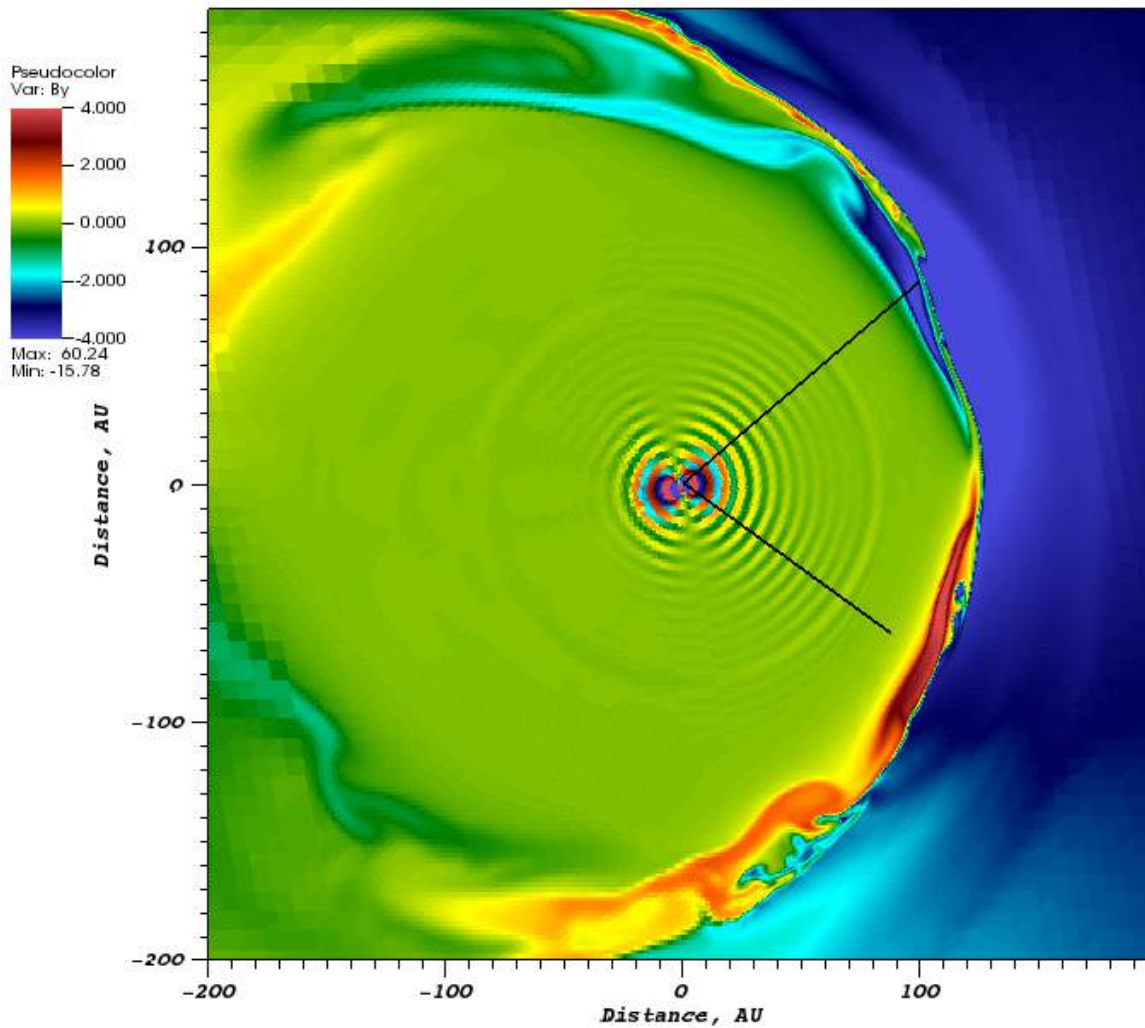


t=3662.540743649215983168688 step=62200

Borovikov & Pogorelov (2014)



V1V2 Plane



V1V2 Plane

INTERSTELLAR WAKE OF SOLAR WIND

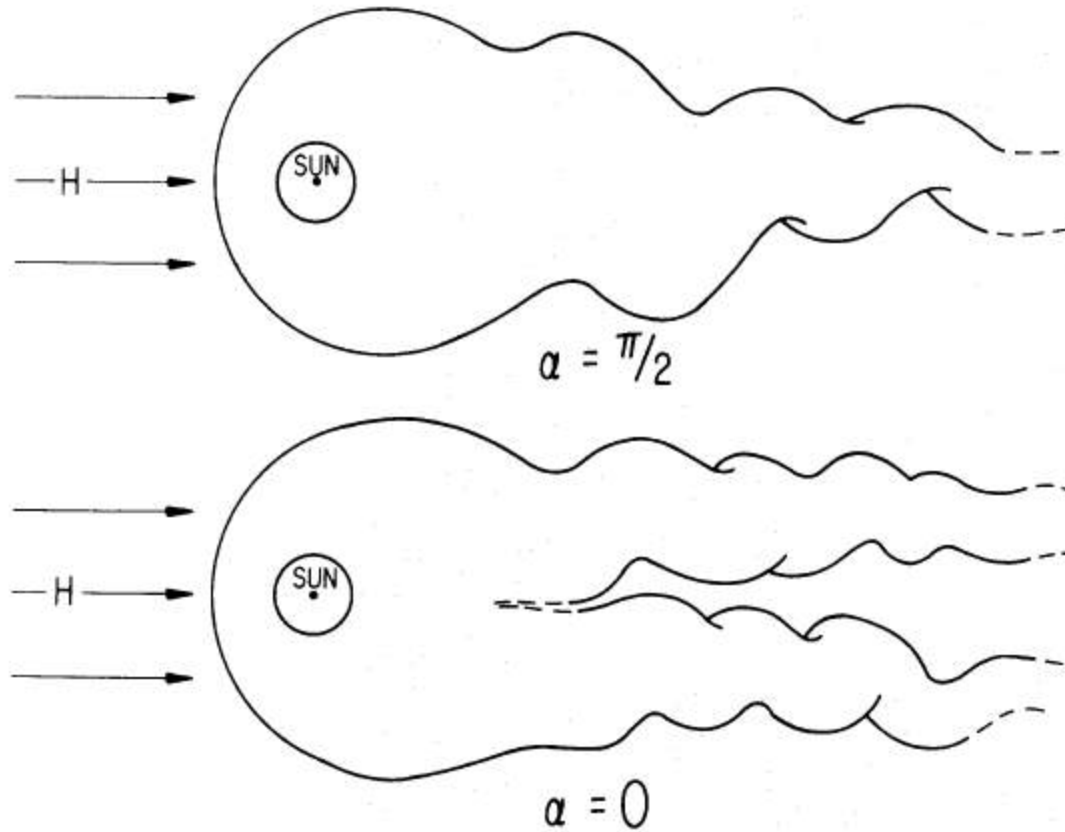
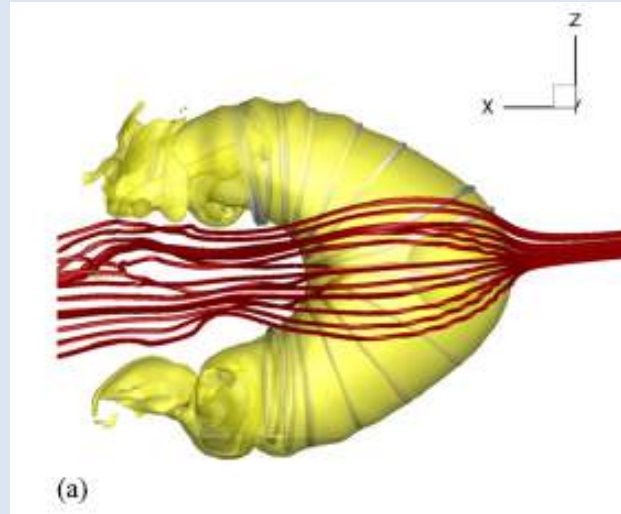
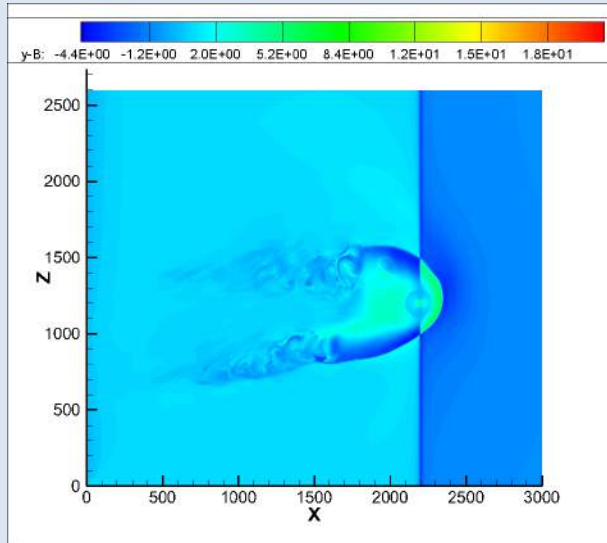


FIG. 7.—The buckling of the solar wind wake

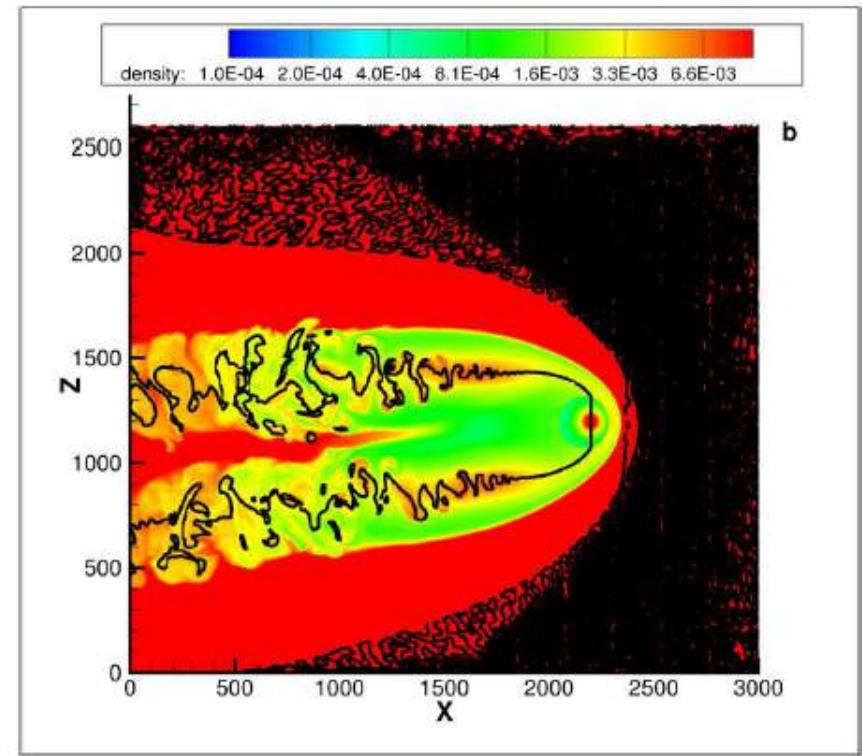
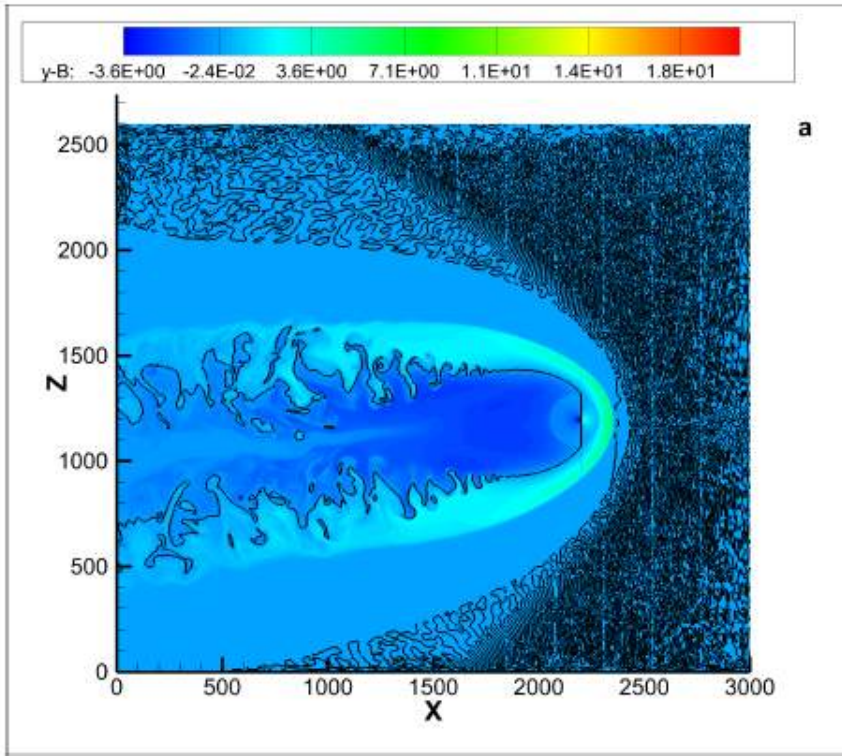
From Yu (1974)

Simulations with the Boundary Conditions from Opher et al. (2015): Unipolar HMF Model, or Why Would the SW have a two-lobe structure?

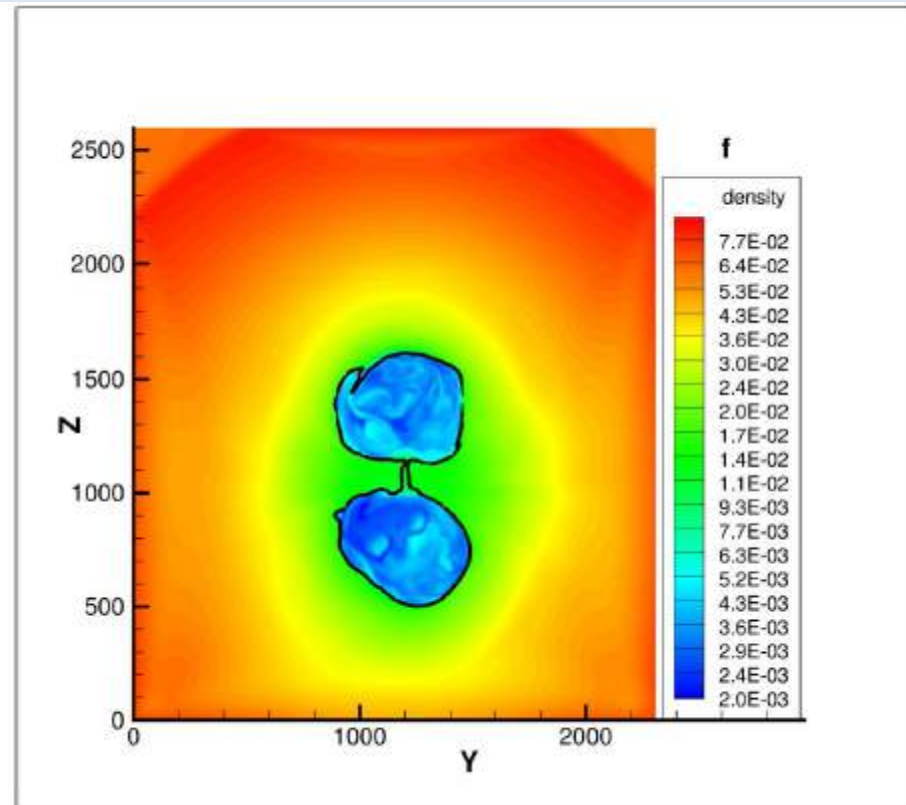
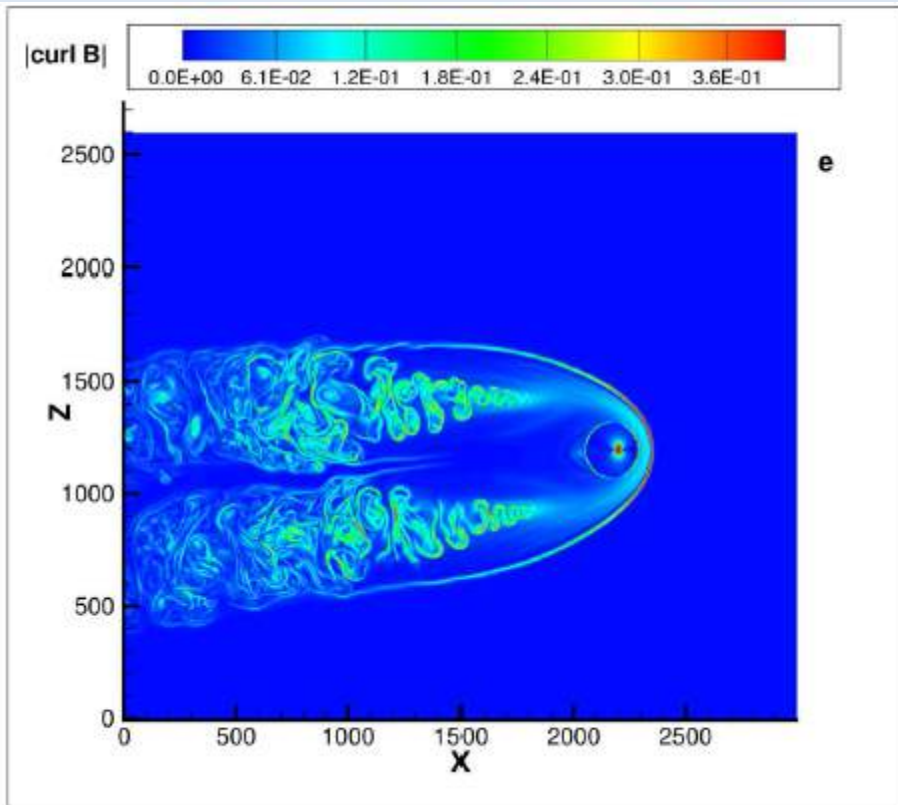


The toroidal component of magnetic field is similar to multi-fluid simulations of Opher et al. (2015). This feature disappears when neutral atoms are treated kinetically.

Our simulations (Pogorelov et al. 2015) with parameters from Opher et al. (2015) with $B_{ISM}=0$

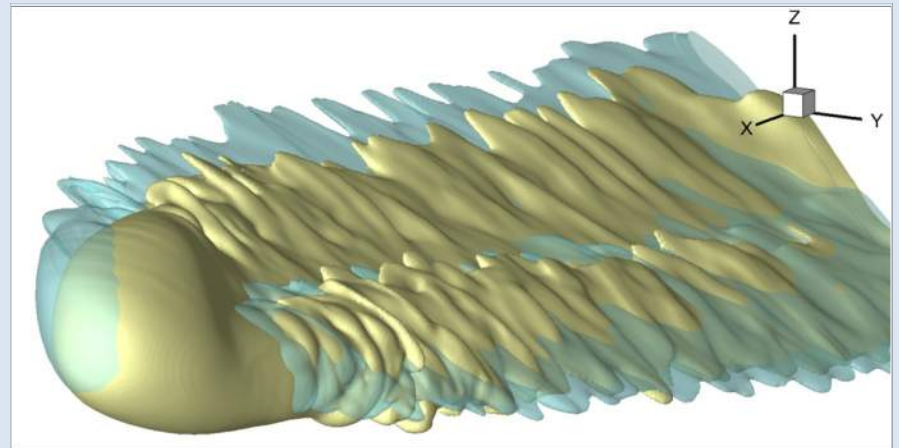
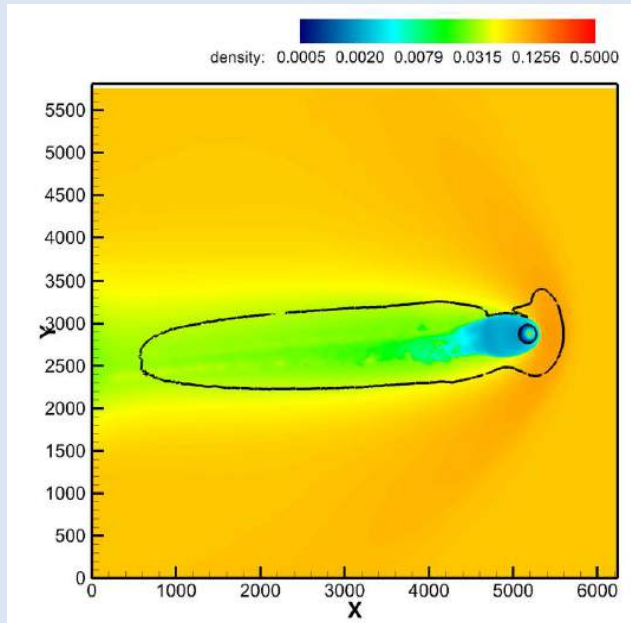


B_y (left) and plasma density (right) in the meridional plane. The black line inside the HP is defined by $B_y=0$ - the effective center of deflected (initially Parker) spiral field.



**Curl of B (left) in the meridional plane and plasma density at $x=200$ (right).
The black line outlines the HP.**

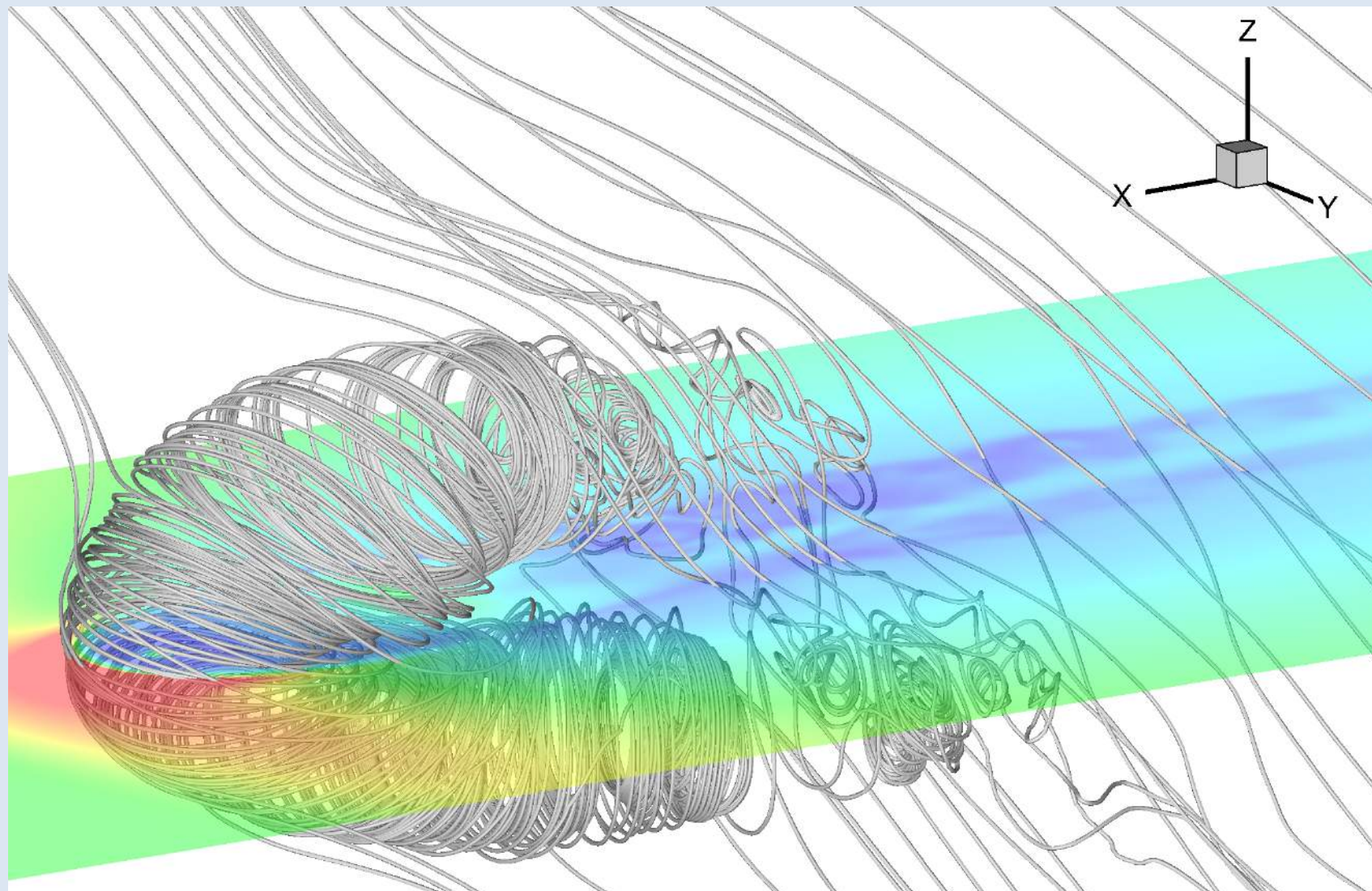
5000 AU heliotail with the unipolar IMF and kinetic treatment of H atoms (Pogorelov et al., 2015)



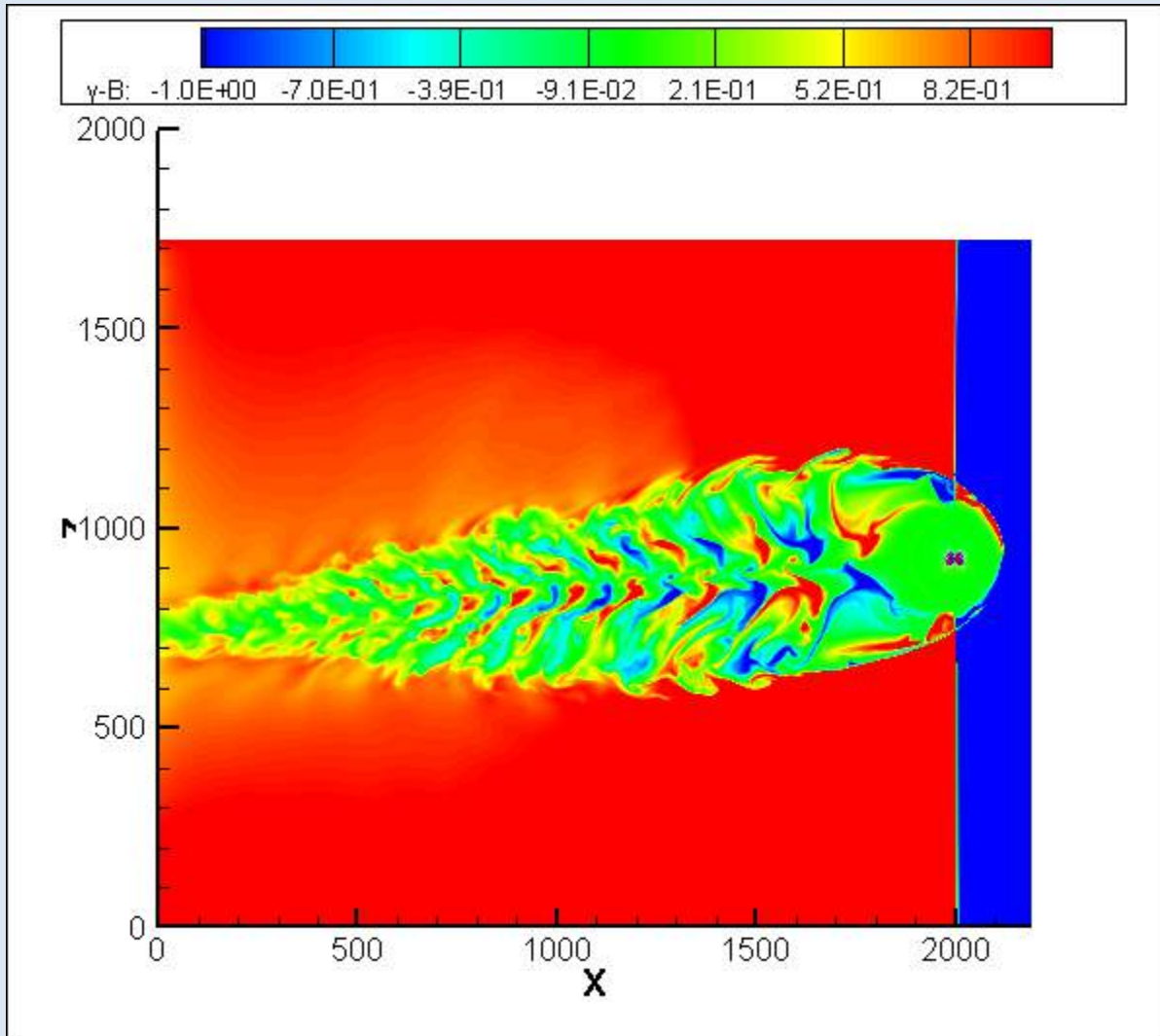
Plasma density in the solar equatorial plane. The black line is defined by the condition $M_f=1$.

Pogorelov et al. (2013): the HP for $B_\infty = 3 \mu\text{G}$ (yellow) and $B_\infty = 4 \mu\text{G}$ (blue): no two-lobe structure in agreement with Izmodenov et al. (2015).

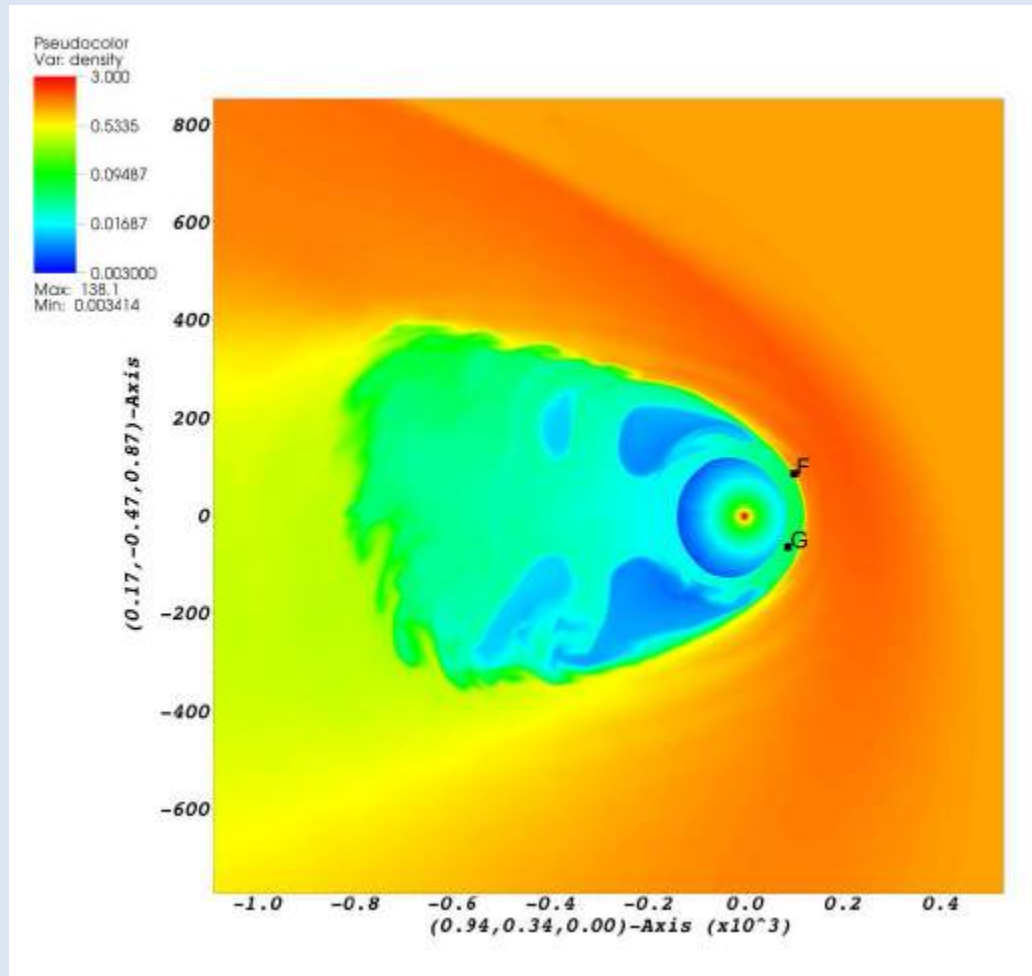
HMF and ISMF lines: the regular Parker field is destroyed in the tail



The shift of the heliotail may give more information on the ISMF direction through fitting TeV GCR small-scale anisotropy (Zhang et al. 2014)



The y- (out-of-plane) component of the magnetic field shows features of solar cycle.



Plasma density in the V1-V2 plane and the spacecraft positions on January 1, 2015. The HP is at 126 AU in the V1 direction and at 128 AU in the V2 direction. With some scaling, V2 will possibly cross the HP in 5 years.

Conclusions

1. The combination of SOHO, IBEX, Voyager, and air shower observations provides us with a powerful tool to constraint the properties of the LISM.
2. Combining macro- and micro-scales is essential for the explanation and interpretation of observational data.